NANOTECHNOLOGY IS AN increasingly hot innovation topic, basing its significance on the foresight that it will fuel countless future advances in materials science, biomedical science, and environmental science [1], [2]. With promises of broad benefits for mankind, nanotech activities are being pursued in many engineering disciplines and branches of industry. Breakthroughs in the area of materials science are emerging with respect to the enhanced control of many physical materials properties. Nanotechnology in biology and medicine is currently at the leading edge of rapid developments in the improvement of technologies for the early detection, diagnosis, control, and treatment of specific diseases. Future progress in developing sustainable and cost-effective technologies for soil, water, and air purification, as well as for renewable energy generation, is also expected to increasingly depend on innovations in the nanotechnology domain. The current economic significance of the nanotech industry and its expected future development are discussed in detail in [3].

Apart from the benefits associated with the growth of the nanotechnology domain, there are legitimate concerns about the potential consequences to our health and environment associated with exposure to nanomaterials, in particular to nanoparticles (NPs) sized smaller than about 0.1 μm [2]. Many water-insoluble solid NPs are suspected to be intrinsically toxic, although quantitative data are still scarce and much remains unknown [4], [5]. Human exposure to NPs occurs via the gastrointestinal tract, the skin, direct injection in the course of a medical treatment, and the respiratory tract by inhaling air that is polluted with airborne NPs. It is widely accepted that NP intake the respiratory tract is the most significant exposure route. Here, the potential risk to the health of workers employed by the nanomaterials industry, where products are made that comprise engineered NPs, is of particu-

Nanoparticle Monitoring for Exposure Assessment

Monitoring airborne nanoparticles creates awareness and enables control.

JOHAN MARRA, WILLEM VAN DEN BRINK, HENK GOOSSENS, AND SJOERD KESSELS

lar concern because exposure levels will usually be highest during the manufacturing stage.

Exposure to engineered NPs has an obvious relation with the exposure to

> Epidemiological studies cannot disentangle the separate effects of UFPs and FPs; however, many toxicological studies indicate an increasing particle toxicity per unit mass when the particle size decreases.

similar sized anthropogenic ultrafine particles (UFPs; $< 0.3\,\mu$m). UFPs are the incidental products of a variety of processes and activities that usually involve combustion and heating. Automobile traffic is a main source of UFPs and other pollutants and is responsible for a significant part of the ambient air pollution level. UFPs constitute a subclass of the total particulate matter (PM) air pollution burden, wherein all airborne fine particles (FPs) smaller than about

$10\,\mu$m are accounted for (PM_{10}), with increasing emphasis on the particles smaller than $2.5\,\mu$m $(PM_{2.5})$. Epidemiologic studies have established a clear link between the ambient FP air pollution level and adverse health effects associated with cardiovascular and respiratory diseases with distinct short- and long-term latent effects [6]–[10]. These become particularly pronounced in susceptible groups of the population such as asthmatics, patients with chronic obstructive pulmonary disease (COPD), the elderly, and infants. Epidemiological studies cannot disentangle the separate effects of UFPs and FPs; however, many toxicological studies indicate an increasing particle toxicity per unit mass when the particle size decreases [5].

Insights from epidemiological studies are useful to guide investigations with respect to the hazards and risks of engineered NPs, but it is certainly not justified to simply equate the toxicity of engineered NPs with the toxicity of ambient UFPs. The hazard of particles is associated with their surface chemistry, chemical composition, size, catalytic activity, morphology, and shape. Because engineered NPs may differ from ambient UFPs in one or more of these aspects, their hazard can be quite different [2]. This uncertainty is of concern in view of the prediction that, in five to ten years from now, the number of manufacturing jobs in the worldwide nanotech industry will increase

to about 10% of all manufacturing jobs [3]. Admittedly, actual exposure to airborne nanomaterials will be relevant to only a limited percentage of the workers in these jobs; however, this will then still affect millions of people.

When the hazard of a certain engineered NP is unknown, precautionary measures aiming at exposure minimization are recommended in workplaces wherein NPs are handled or processed. In parallel, a continuous control of the ambient air NP pollution level is advocated, preferably by monitoring both the workplace NP pollution level and the cumulative personal exposure to airborne NPs. This calls for the use of an NP monitor capable of yielding an output signal, which is proportional to a metric that is relevant for assessing both the NP and the ambient UFP exposure levels and the relative health risk associated with those exposures. The Aerasense NP monitor, discussed in this article, is capable of doing just that in a unique way that cannot be accomplished with the existing commercial equipment. Its functionality accounts for the deposition pattern of airborne particles in the respiratory tract and their subsequent behavior, while being embodied such as to satisfy practical demands concerning the portability, cost, and robustness of a NP monitor.

In what follows, the deposition behavior of inhaled NPs in the respiratory tract will be discussed in more detail, followed by an explanation of the design and operation of the Aerasense NP monitor. Its response in a number of relevant environments wherein the air is polluted to various degrees with NPs or UFPs will be illustrated, thereby highlighting the application scope of the Aerasense NP monitor both indoors and outdoors.

NANOPARTICLE EXPOSURE AND HEALTH RISKS

The health risk R associated with NP exposure is proportional to the product of the toxicological hazard H and the exposure level E according to
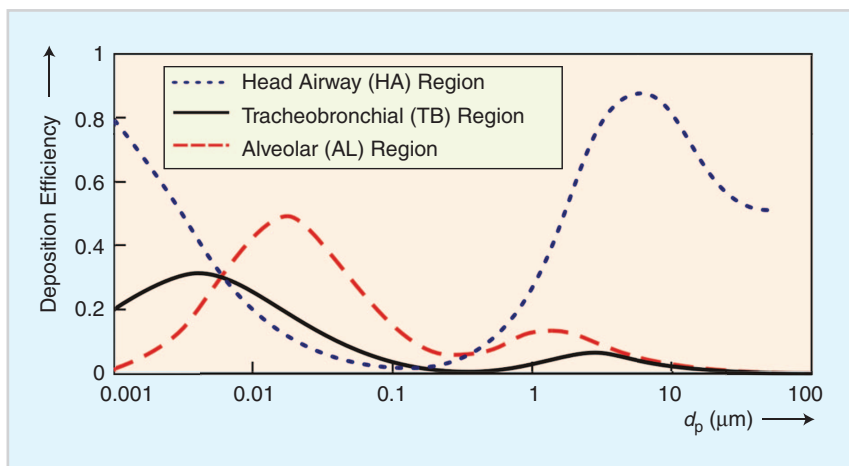
$$R \propto H*E. \qquad (1)$$

FIGURE 1 Fractional deposition efficiency of inhaled airborne particles in the various regions of the respiratory tract as a function of their diameter d_p according to the ICRP model for a reference worker [14].

The particle hazard must be separately established for each kind of particle. Toxicologists usually express exposure in terms of a mass concentration; however, there is increasing evidence that exposure to solid water-insoluble NPs is more appropriately expressed in terms of the NP number concentration N or the NP surface area concentration S [5]. More in particular, the fraction S_{dep} of the total particle surface area concentration in the inhaled air that actually deposits in the respiratory tract has been recognized as a relevant exposure metric, because the interaction between the body and the deposited particles occurs primarily via their surfaces and

the reactive chemical groups thereon [11]–[13].

The direct physical reason underlying the health risks associated with NP and UFP inhalation comes from their ability to reach and deposit in all parts of the respiratory system. Figure 1 depicts the deposition efficiency of the inhaled particles as a function of their diameter d_p in the upper head airway (HA) region, the tracheobronchial (TB) region, and the deep alveolar (AL) region of the respiratory tract where gas exchange with the blood occurs [14]. The results in Figure 1 correspond with the deposition model of the International Commission of Radiological Protection (ICRP) for a
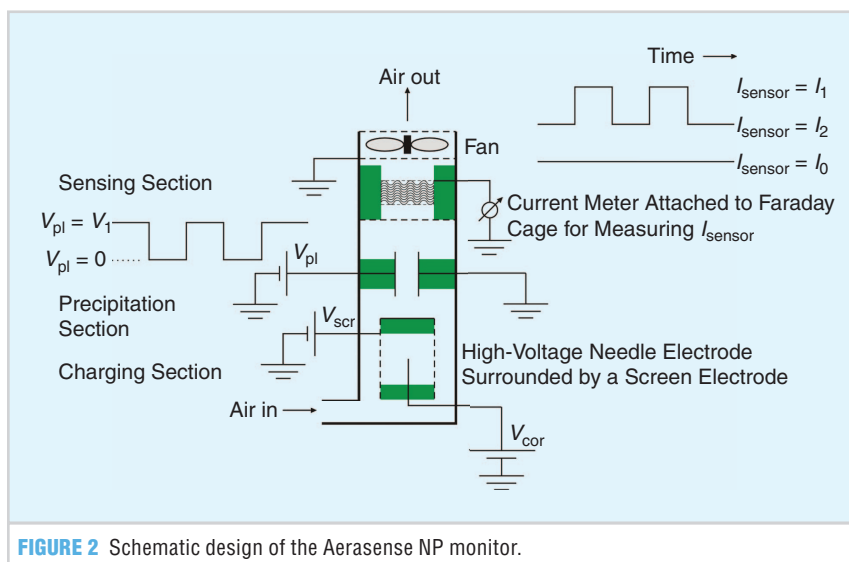

FIGURE 2 Schematic design of the Aerasense NP monitor.

FIGURE 3 The Aerasense NanoTracer.

reference person who is breathing according to a set of specified conditions and highlight the distinct effect of the particle size on the particle deposition beyond the head-airways for all particle sizes $d_p \leq 10\,\mu m$. The very slow clearance of particulates from the alveolar region has been associated with local tissue inflammation that is believed to initiate and aggravate a variety of respiratory diseases. NPs deposited in the nose may create additional (as yet unknown) risk through their potential ability to transfer to the brain via the olfactory nerve [15]. Translocation of the deposited NPs from the lung alveoli to extrapulmonary sites, such as the systemic circulation, the heart, and the spleen, has been demonstrated, thereby providing backup evidence that inhaled NPs can play a role in the triggering and promotion of cardiovascular morbidity and mortality [2].

Based on the earlier discussion, a NP monitor should yield information about the particle surface area concentration per unit volume of inhaled air that deposits in the various compartments of the respiratory tract. In addition, it is desirable to have information about the particle number concentration and the encountered particle sizes to better characterize the ambient NP pollution level.

DESIGN AND OPERATION OF THE AERASENSE MONITOR

Figure 2 schematically depicts the layout of the Aerasense monitor. Its operation relies on particle charging and the measurement of the total particle charge per unit air volume. For this purpose, a controlled airflow ϕ is drawn through the monitor by means of a fan situated atop of the sensor. After entry, airborne particles are electrically charged inside the charging section via diffusion charging [16]. Diffusion charging is enabled by a corona discharge from a needle-tip electrode that is set at a sufficiently high voltage V_{cor} to locally ionize the air. The needle-tip electrode is surrounded by a screen electrode whereupon a screen voltage $V_{scr} \ll V_{cor}$ is imposed. Particle charging occurs in the air conduit between the screen electrode and the opposite earthed wall by contacting the particles with ions that move from the screen electrode across the conduit toward the wall. Charging conditions are chosen such that the average particle charge $Q(d_p)$ on a particle of diameter d_p is directly proportional to d_p, i.e., $Q(d_p) \propto d_p$.

After charging, the particles enter the precipitation section wherein a block-shaped voltage pulse varying between $V_{pl} = V_1$ and $V_{pl} = 0$ is imposed between two parallel electrode plates separated by a distance d_{pl}. At $V_{pl} = 0$, charged particles traverse the precipitation section unhindered. They are subsequently captured in a particle filter disposed inside an electrically isolated Faraday cage that is connected via a sensitive current meter to a reference potential. The current meter records the total particle charge that deposits per unit time inside the Faraday cage as an electrical current $I_{sensor} = I_1$. The current I_{sensor} constitutes the sensor signal. At $V_{pl} = V_1$, at least some charged particles precipitate inside the precipitation section due to the field strength $E_{pl} = V_1/d_{pl}$ between the plates. All remaining particles are subsequently captured inside the Faraday cage, giving rise to a second sensor signal I_2. Obviously, $I_2 < I_1$. Provided that E_{pl} remains sufficiently low to only partly precipitate all particles of any

FIGURE 4 The Aerasense Nano-Monitor.

> The direct physical reason underlying the health risks associated with NP and UFP inhalation comes from their ability to reach and deposit in all parts of the respiratory system.

size that contribute to a nonnegligible extent to the total particle number concentration, it can be shown that the total particle number concentration N and the number-averaged particle size $d_{p,av}$ relates to I_1 and I_2 according to

$$N = S_N(I_1 - I_2), \qquad (2)$$
$$d_{p,av} = S_{dp}\frac{I_1}{I_1 - I_2}, \qquad (3)$$

wherein S_N and S_{dp} are constants that appear to be rather insensitive to the details of the particle size distribution within the $0.01 - 0.30\,\mu m$ particle size domain [17]. Combining (1) and (2) relates the signal I_1 to the particle length concentration L according to

$$L = Nd_{p,av} = S_N S_{dp} I_1. \qquad (4)$$

Although a broad range of airborne particles size may be present, the contribution of particles in the $0.01–0.30\,\mu m$ size range to the sensor signals I_1 and I_2 is almost always dominating because the particle number concentration for $d_p < 0.3\,\mu m$ is normally much higher than for $d_p > 0.3\,\mu m$. This makes the Aerasense monitor to effectively perform as a NP or UFP monitor.

In ambient outdoor and indoor air, the usual situation is that $0.025\,\mu m \le d_{p,av} \le 0.10\,\mu m$. Taking a default average diameter $(d_{p,av})_{def} = 0.05\,\mu m$, it becomes possible to infer an apparent particle number concentration N_{app} from (4) according to

$$N_{app} = \frac{S_N S_{dp} I_1}{(d_{p,av})_{def}}, \quad (5)$$

which will be accurate to within, at worst, a factor of 2. Note that for a mere evaluation of N_{app} it is not required to incorporate a precipitation section in the monitor shown in Figure 2.

An assessment of the deposited particle surface area S_{dep} per unit volume of inhaled air in some region of the respiratory tract follows from

$$S_{dep} = \int_{dp=0}^{\infty} \pi d_p^2 D(d_p) d(N(d_p)), \quad (6)$$

wherein $D(d_p)$ represents the particle deposition efficiency as a function of particle size in that region of the respiratory tract, as drawn in Figure 1 for the HA, TB, and AL regions, and $N(d_p)$ the concentration of particles of size d_p [14]. For a broad range of particle size distributions, it was discovered that S_{dep} scales linearly with both N and $d_{p,av}$ for all regions up to an accuracy of about 15–25% provided that $0.025\,\mu m \le d_{p,av} \le 0.08 - 0.10\,\mu m$ [17]. Specifically, with S_{dep} expressed in $\mu m^2/cm^3$, N in particles/cm^3 and $d_{p,av}$ in μm, it can be derived that

$$S_{AL}(N, d_{p,av}) \approx 5.4*10^{-2} N d_{p,av} \propto I_1,$$
$$S_{TB}(N, d_{p,av}) \approx 1.0*10^{-2} N d_{p,av} \propto I_1,$$
$$S_{HA}(N, d_{p,av}) \approx 0.6*10^{-2} N d_{p,av} \propto I_1.$$
$$(7)$$

As mentioned earlier, it is believed that, in particular, $S_{AL} \propto N d_{p,av}$ is a useful metric for assessing the relative exposure-induced health risk at a given particle hazard. Equation (7) shows that the sensor signal I_1 is directly proportional to this incurred health risk. In case the particle hazard is known from the toxicological experiments, it becomes

possible to estimate a safe concentration limit $(N d_{p,av})_{ref}$ below which no adverse health effects are to be expected. Actually encountered NP concentrations can then be compared with $(N d_{p,av})_{ref}$ and measures and warnings issued accordingly.

The earlier discussion indicates the capability of the Aerasense monitor to assess the characteristics of the NP pollution level in terms of N and $d_{p,av}$ and to produce a signal I_1 or, equivalently, an inferred apparent particle concentration N_{app} according to (5) that is directly proportional to the relative exposure-induced health risk.

REALIZATION OF THE AERASENSE MONITOR
The Aerasense monitor is either embodied as a battery-powered hand-held device (NanoTracer, see Figure 3) or as a mains-powered wall-mount device (NanoMonitor, see Figure 4).

The NanoTracer is designed according to the layout shown in Figure 2,

and is therefore capable of providing real-time information about the NP or UFP air pollution characteristics $(N, d_{p,av})$ and about the relative health risk associated with NP or UFP inhalation (via I_1, N_{app}, or S_{AL}). Measured data are updated once every 10 s and are internally logged to enable subsequent downloading and analysis on a PC. The manual pressing of the MARK button can be used to mark a moment in time at which, for instance, an event occurred that could affect the airborne NP concentration level. An automatic zero-check is periodically carried out to compensate for possible signal drifts in the course of time. This zero-check can also be manually activated and involves a stopping of the airflow through the monitor. A zero airflow through the monitor must correspond with a zero sensor signal. Its portability enables the NanoTracer to be used for measuring while walking around and for a rapid tracing of NP-emitting sources. The NanoTracer can
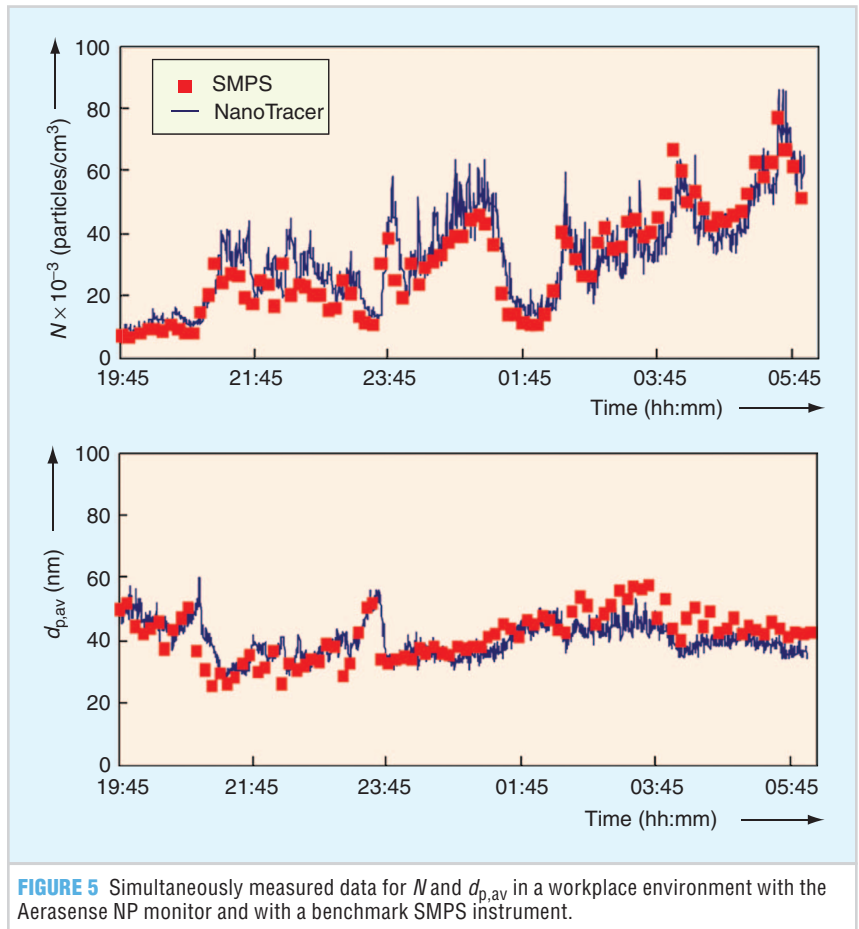
FIGURE 5 Simultaneously measured data for N and $d_{p,av}$ in a workplace environment with the Aerasense NP monitor and with a benchmark SMPS instrument.

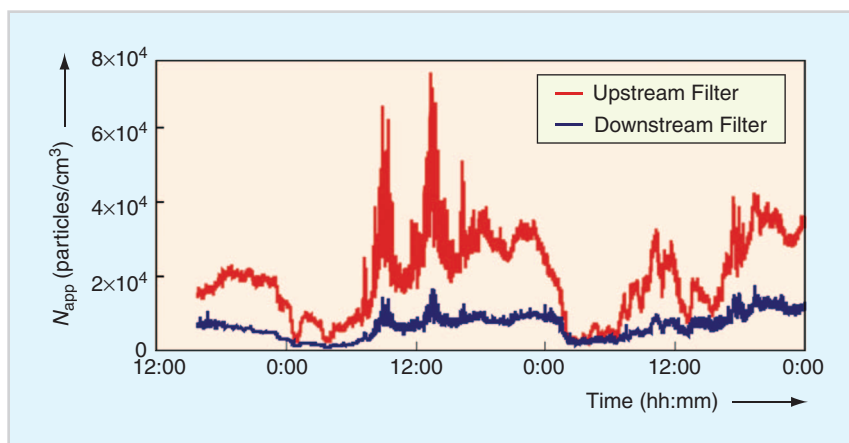**FIGURE 6** Simultaneously measured data for N_{app} upstream and downstream of a F7 particle filter inside a building ventilation unit during several days.

be attached to a belt around a person's waist and equipped with a sampling tube to continuously sample air from the breathing zone of a worker. Both the momentary and cumulative exposures of this person to NPs during a workshift can then be obtained. Such information is useful to evaluate the overall effectiveness of exposure minimization measures and to compare the incurred cumulative exposure to a possible set maximum cumulative exposure level.

The NanoMonitor is similar to the NanoTracer but does not make use of the precipitation section shown in Figure 2 and is therefore only capable of generating the sensor signal I_1. Knowledge of I_1 is sufficient to infer an apparent particle number concentration N_{app} according to (5), which is proportional to the incurred relative

health risk associated with NP inhalation. Measurements can be updated as fast as once in every 4–5 s. The Nano-Monitor generates an analogue output signal, which can be used for enabling a variety of functionalities including the feedback control of air handling units, the checking of the performance of installed filtration units, and for informing people about the ambient airborne UFP pollution level, thus creating awareness. The NanoMonitor may be incorporated in a building management system.

MEASURING WITH THE AERASENSE MONITOR

IN A WORKPLACE
An example of a measurement with the Aerasense NP monitor in a nanotech

workplace environment, ventilated with filtered outdoor air, is shown in Figure 5. Here, a pilot-type NP manufacturing process was carried out in a closed chemical reactor vessel. It was discovered during process operation that the presence of several red-hot heated surfaces exposed to air acted as a major NP source creating a relatively high NP pollution level comprising NPs of unknown toxicity. At the same time, parallel particle sampling and particle analysis experiments did not indicate the escape of engineered NPs from the reactor vessel; thus, ambient airborne NPs were mostly inadvertently released secondary particles from the process equipment. Figure 5 presents a series of data for both N and $d_{p,av}$ measured with the Aerasense NP monitor and, independently, with a Scanning Mobility Particle Sizer (SMPS; Type #5403; Grimm GmbH, Germany). The SMPS is a benchmark professional aerosol analysis instrument capable of recording N and the particle size distribution $N(d_p)$ in the $11\,\text{nm} \leq d_p \leq 1083\,\text{nm}$ particle size interval. It is a high-cost heavy instrument equipped with a radioactive source for aerosol charge neutralization. Agreement of the measured data for N and $d_{p,av}$ with both instruments in the course of time is very good, thereby verifying the reliability of the Aerasense monitor. It is clear from the presented data that transients in the NP air pollution level can be more easily resolved with the NP monitor than with the SMPS: the SMPS updates its measurements once every 6 min while the Aerasense monitor does so once every 10 s. These workplace measurements illustrate the capability of the Aerasense monitor to quickly gauge some key characteristics of the NP air pollution level and to trace the NP pollution sources.

IN A BUILDING
An example of a three-day measurement of N_{app} in an air-handling unit on the top floor of one of the Philips Research buildings in Eindhoven is shown in . This air-handling unit continuously draws outdoor air as ventilation air into the building, thereby passing this air through a panel-type
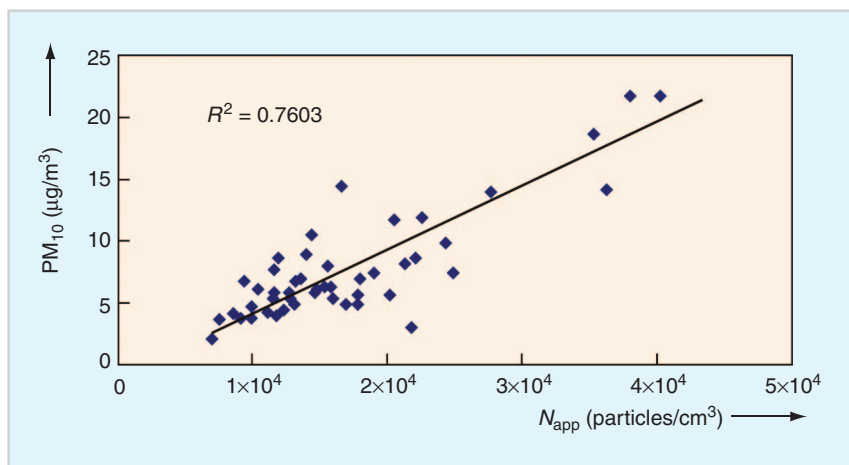

FIGURE 7 Comparison between simultaneously measured data for PM_{10} and N_{app} in ventilation air drawn from outdoors.

minipleated F7 particle filter. Two Aerasense NP monitors were used to simultaneously measure N_{app} upstream and downstream of the F7 filter. This filter is a commonly used ventilation air filter and is capable of removing 50–70% of the airborne UFPs during a single pass (Figure 6). It is expected that the filtration efficiency for larger airborne particles $(d_{p,av} \geq 0.5 \mu m)$ is even better because all mechanical dust filters are known to have a minimum efficiency in the 0.1–0.2 μm particle size region [18]. It is clear from Figure 6 that even within a single day, the outdoor UFP pollution level can vary by more than an order of magnitude, depending on environmental conditions, such as weather and wind speed. During periods of smog, the UFP concentration level can rise up to $N_{app} = 100,000 - 200,000$ particles/cm^3, requiring a very significant degree of filtration to bring the indoor N_{app} down to $N_{app} < 5,000 - 10,000$ particles/cm^3 required to accomplish clean indoor air conditions. In contrast, rainy and windy weathers can lead to an outdoor $N_{app} < 2,000 - 5,000$ particles/cm^3; thus, a very low outdoor UFP pollution level might make any air filtration unnecessary.

Of course, the overall air cleanliness also involves the particulate pollution with FPs in the $0.3 - 10 \mu m$ particle size interval. In this context, it was investigated whether any relationship exists between the outdoor UFP number concentration N_{app} (effectively representing particles with $d_p < 0.3 \mu m$) and the outdoor PM$_{10}$ concentration, the latter representing mostly the mass concentration of all airborne FPs with $d_p \leq 10 \mu m$. Such a comparison is of interest because current (outdoor) air pollution regulations only involve the PM$_{10}$ concentration level. The regulation is that the particulate air pollution level is deemed satisfactory as long as the annual average PM$_{10} < 40 \mu g/m^3$. Figure 7 shows the results of parallel outdoor measurements of N_{app} and PM$_{10}$, each measured point representing a value averaged more than a 12-h period. Measurements were performed at a location
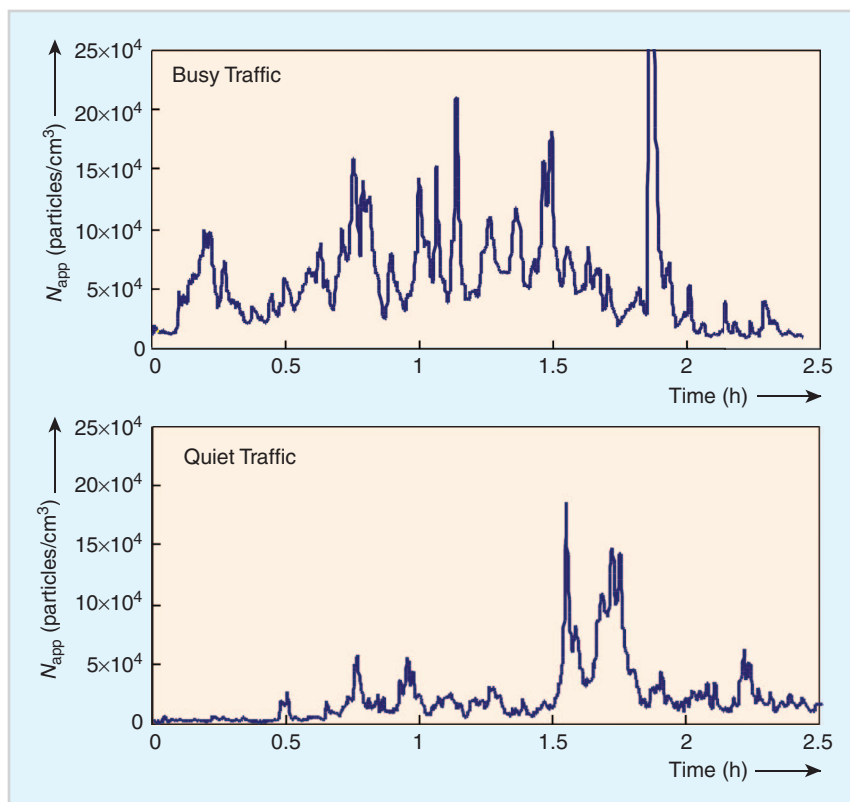

FIGURE 8 Measurements of N_{app} in a car cabin during driving under both busy and quiet traffic conditions.
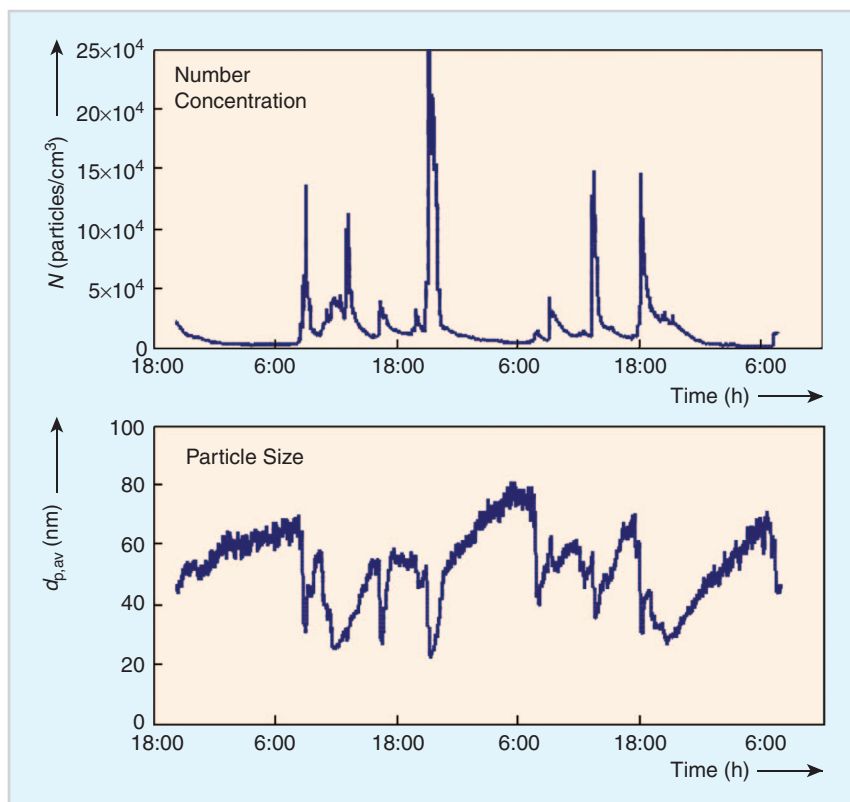

FIGURE 9 Simultaneously measured values for N and $d_{p,av}$ in a poorly ventilated home environment during a two-day period.

remote from the direct proximity of particle sources like motorized traffic, thus yielding background concentration levels. It is clear that, with some scatter, there is indeed a positive correlation between N_{app} and PM_{10}, which can be understood from the circumstance that PM_{10} particles originate at least partly from the same sources as UFPs. Therefore, a low UFP background concentration level will often also indicate a low PM_{10} background concentration level. This inference supports the statement that the result of a UFP measurement in outdoor air can often be sufficient for assessing the outdoor air quality with respect to particulate pollution. On the other hand, no clear relationship between the UFP and FP concentration levels was found indoors: many indoor particle sources (cooking, candle burning, smoking, vacuum cleaning, etc.) emit both FPs and UFPs, but different particle sources are often characterized by widely different FP or UFP concentration ratios.

Using NP monitors for monitoring pollution levels in both outdoor and indoor air enables the implementation of a smart air-handling strategy that explicitly takes the indoor and outdoor UFP concentration levels into account as additional decision parameters to balance indoor air quality requirements with the air-handling unit's energy consumption needs and any possibly imposed energy budget constraints. Any air-handling strategy will normally have to deal with imposed ventilation, filtration, heating, cooling, and humidification requirements, and therefore, its control relies also on additional inputs from temperature and humidity sensors. An augmented strategy that also accounts for the indoor UFP concentration level could bring more sophistication in the realization of demand-controlled ventilation, demand-controlled filtration (depending on the ambient outdoor UFP pollution level), ventilation flow control, indoor air recirculation control, and heat recovery. In addition, the use of NP monitors allows for an easy check on the filtration efficiency of air cleaning units.

> Automobile driving occurs mostly in the midst of many other vehicles that all act as UFP sources. Currently used cabin air filters were found to be effective only for arresting comparatively large particles such as pollen from the air.

IN AN AUTOMOBILE

Another location wherein the ambient UFP concentration plays an important role is inside the cabin of automobiles. Automobile driving occurs mostly in the midst of many other vehicles that all act as UFP sources. Currently used cabin air filters were found to be effective only for arresting comparatively large particles such as pollen from the air. Measurements of N_{app} in Figure 8 were recorded during two driving episodes of 2.5 h each, one on a Friday afternoon during busy traffic conditions (outdoor off-road $N_{app} \approx 20,000$ particles/cm^3) and one on a Sunday afternoon when traffic conditions were quiet (initial outdoor ambient $N_{app} \approx 1,000 - 2,000$ particles/cm^3 near the sea). It is clear that busy traffic conditions induce a significantly increased average cabin UFP concentration level that far exceeds the off-road ambient level. This is particularly relevant for the health and well-being of professional drivers who are on the road for many hours each day. One way to solve this would be to install an improved cabin filter; however, this appears to be not easily feasible given the strict constraints imposed on the automobile's air handling system concerning cost, size, minimum required airflows, maximum allowed power consumption, and the minimum required heating or cooling performance. A simple closing of the car's ventilation air intake is not recommended because of the ventilation needs to remove moisture, odors, gases, and CO_2. Here,

a better solution is foreseen with a NP monitor capable of continuously recording the cabin's UFP pollution level. Feedback from the NP monitor in response to the measured cabin's UFP concentration can then be used to optimize the settings of the vehicle's air-handling unit with respect to the total airflow, the degree of cabin air-recirculation through the air filter, and the volumetric intake of outdoor air. This strategy allows for a better tuning of the car's air-handling system, taking into account not only the cabin's heating and cooling requirements but also the cabin air cleanliness.

IN A HOME

Many people reside most of their time in their own homes, and it is, therefore, worthwhile considering the indoor UFP pollution level to which they are exposed. UFPs are present in the ventilation air drawn from outdoors, and this can be particularly serious in polluted cities, but are also generated indoors due to human activities such as smoking, cooking, frying, heating, vacuum cleaning, and candle burning. An example of the measured UFP concentration characteristics in a home relying on natural ventilation during a two-day period is presented in Figure 9. The natural ventilation was always kept at a very low level except when significantly elevated UFP pollutions were recorded at which time a window was opened to quickly reduce the indoor pollution level. In the absence of nearby car traffic, the outdoor air was quite clean with a UFP concentration $N \approx 5,000$ particles/cm^3 throughout the measurement period. Figure 9 shows that high UFP pollution peaks indeed occur as a result of ordinary daytime activities such as cooking or frying, vacuum cleaning (involving the operation of an electric carbon brush motor that releases carbon NPs), and steam ironing. Average sizes of the freshly produced UFPs were typically in the range of 20–30 nm. During the night, a slow decrease of N was observed in parallel with a gradual increase in $d_{p,av}$. This is attributed to particle coagulation. In any case, natural ventilation was found to be an excellent strategy to quickly remove

polluted air from indoors when the outdoor air is cleaner. The use of one or more NP monitors in a home could be worthwhile for automatically triggering the demand-controlled ventilation in case the home is provided with mechanical ventilation or for signaling the residents to increase the natural ventilation level when necessary. Ideally, a recording should be made of both the outdoor and the indoor UFP concentrations. A NP monitor can then assist in optimizing ventilation levels such as to realize a satisfactory indoor air quality at a minimum expense of energy. Evidently, such an optimization will also have to rely on input from temperature and humidity sensors and an energy meter.

CONCLUSIONS AND PROSPECT

Particulate air pollution comprising inhalable particles with $d_p \leq 10 \mu m$ is an important determinant of the severity of the overall air pollution level. Among these, the airborne UFPs and NPs with $d_p \leq 0.1 - 0.3 \mu m$ form a particular class of particles because of recent insights that the particle toxicity per unit particle mass is inversely proportional to the particle size. The toxicity of many engineered NPs is thereby still unknown, thus mandating precautionary measures to reduce personal exposure. In this context, the Aerasense NP monitor is a useful instrument to promote human awareness about the issue of NP pollution, to assess personal exposure, to trace pollution sources, and to monitor the effect of exposure reduction measures. Its output signals allow for a characterization of the encountered NP/UFP pollution level and for a generation of a signal that is foreseen to directly relate to the incurred inhalation-induced health risk. In addition, the NP monitor can be used for early warning purposes and for feedback to actively control the settings and operation of air-handling units and air-cleaning units. This can be used to ensure that the NP or UFP pollution levels remain at all times below certain set concentration levels and that the strategy with which this is done is carried out such that the required energy consumption is minimized. Judicious compromises can then be made between the optimization of the indoor air quality in a variety of environments on the one hand and the incurred energy costs on the other hand.

ABOUT THE AUTHORS

Johan Marra (johan.marra@philips.com) is a principal scientist at Philips Research Laboratories, Eindhoven, The Netherlands.

Willem van den Brink (willem.van.den.brink@philips.com) is a general manager of the Aerasense venture within Philips Research Laboratories, Eindhoven, The Netherlands.

Henk Goossens (henk.goossens@philips.com) is a marketing manager at the Aerasense venture within Philips Research Laboratories, Eindhoven, The Netherlands.

Sjoerd Kessels (sjoerd.kessels@philips.com) is an application engineer at the Aerasense venture within Philips Research Laboratories, Eindhoven, The Netherlands.

Proc. 55th Electronic Components Technology Conf., 2005, pp. 983–987.

[6] P. Lall, S. Islam, J. Suhling, and G. Y. Tian, "Nano-underfills for high-reliability applications in extreme environments," in *Proc. 55th Electronic Components Technology Conf.*, 2005, pp. 212–222.

GENERAL READING

M. P. Allen and D. J. Tildesley, *Computer Simulation of Liquids.* New York: Oxford Univ. Press, 1989.

C. Bailey, H. Lu, S. Stoyanov, T. Tilford, X. Xue, M. Alam, C. Yin, and M. Hughes, "Modelling technologies and applications," in *Nanopackaging: Nanotechnologies and Electronics Packaging*, J. E. Morris, Ed. New York: Springer Verlag, 2008.

ABOUT THE AUTHORS

Chris Bailey (c.bailey@gre.ac.uk) is a professor of computational mechanics and reliability at the University of Greenwich, London. He is also the director of Computational Mechanics and Reliability Group at Greenwich.

Hua Lu (h.lu@gre.ac.uk) is an associate professor in computational science and a member of the Computational Mechanics and Reliability Group at the University of Greenwich.

N

Products *(continued from page 13)*

REFERENCES

[1] M. C. Roco, "Environmentally responsible development of nanotechnology," Environ. Sci. Technol., vol. 39, no. 5, pp. 106A–112A, 2005.

[2] M. R. Gwinn and V. Vallyathan, "Nanoparticles: health effects––Pros and cons," Environ. Health Perspect., vol. 114, no. 2, pp. 1818–1825, 2006.

[3] A. Hullmann, "The economic development of nanotechnology––An indicators based analysis," European Commission, DG Research, Unit S&T, Convergent Science and Technologies, November 28th, 2006. [Online]. Available: ftp://ftp.cordis.europa.eu/pub/nanotechnology/docs/nanoarticle_hullmann_nov2006.pdf

[4] V. L. Calvin, "The potential environmental impact of engineered nanomaterials," *Nat. Biotechnol.,* vol. 21, no. 10, pp. 1166–1170, 2003.

[5] G. Oberdörster, E. Oberdörster, and J. Oberdörster, "Nanotoxicology: an emerging discipline evolving from studies of ultrafine particles," *Environ. Health Perspect.,* vol. 113, no. 7 pp. 823–839, 2005.

[6] A. Nel, "Atmosphere air pollution-related illness: Effects of particles," *Science,* vol. 308, no. 5723, pp. 804–806, 2005.

[7] J. Schwartz, F. Laden, and A. Zanobetti, "The concentration-response relation between $PM_{2.5}$ and daily deaths," *Environ. Health Perspect.,* vol. 110, no. 10 pp. 1025–1029, 2002.

[8] R. J. Delfino, C. Sioutas, and S. Malik, "Potential role of ultrafine particles in associations between airborne particle mass and cardiovascular health," *Environ. Health Perspect.,* vol. 113, no. 8, pp. 934–946, 2005.

[9] D. W. Dockery, C. A. Pope, X. Xu, J. D. Spengler, J. H. Ware, M. E. Fay, B. G. Ferris, and F. Speizer, "An association between air pollution and mortality in six U.S. cities," *New Engl. J. Med.*, vol. 329, no. 24, pp. 1753–1759, 1993.

[10] C. A. Pope, R. T. Burnett, G. D. Thurston, M. J. Thun, E. E. Calle, D. Krewski, and J. J. Godleski, "Cardiovascular mortality and long-term exposure to particulate air pollution: Epidemiological evidence of general pathophysiological pathways of disease," *Circulation,* vol. 109, no. 1, pp. 71–77, 2004.

[11] G. Oberdörster, "Significance of particle parameters in the evaluation of dose-response relationships of inhaled particles," *Particul. Sci. Technol.,* vol. 14, no. 2, pp. 135–151, 1996.

[12] K. Donaldson, X. Y. Li, and W. MacNee, "Ultrafine (nanometer) particle mediated lung injury," *J. Aerosol Sci.,* vol. 29, no. 5–6, pp. 553–560, 1998.

[13] H. Fissan, S. Neumann, A. Trampe, D. Y. H. Pui, and W. G. Shin, "Rationale and principle of an instrument measuring lung deposited nanoparticle surface area," *J. Nanoparticle Res.,* vol. 9, no. 1, pp. 53–59, 2007.

[14] W. C. Hinds, "Respiratory deposition," in *Aerosol Technology: Properties, Behavior, and Measurement of Airborne Particles,* 2nd ed. New York: Wiley, 1998, ch. 11, pp. 233–259.

[15] A. Elder, R. Gelein, V. Silva, T. Feikert, L. Opanashuk, J. Carter, R. Potter, A. Maynard, Y. Ito, J. Finkelstein, and G. Oberdörster, "Translocation of inhaled ultrafine manganese oxide particles to the central nervous system," *Environ. Health Perspect.,* vol. 114, no. 8, pp. 1172–1178, 2006.

[16] M. Adachi, Y. Kousaka, and K. Okuyama, "Unipolar and bipolar diffusion charging of ultrafine aerosol particles," *J. Aerosol Sci.,* vol. 16, no. 2, pp. 109–123, 1985.

[17] J. Marra, "Monitor for detecting and assessing exposure to airborne nanoparticles," in *Proc. Nanosafe2008 Conf.,* Grenoble, France, Nov. 2008, to be published.

[18] R. C. Brown, *Air Filtration.* New York: Pergamon, 1993.

N